JACS
JOURNAL OF THE AMERICAN CHEMICAL SOCIETY
Article
pubs.acs.org/JACS

From a Zwitterionic Phosphasilene to Base Stabilized Silyliumylidene-Phosphide and Bis(silylene) Complexes

Nora C. Breit,[†] Tibor Szilvási,[‡] Tsuyoshi Suzuki,[†] Daniel Gallego,[†] and Shigeyoshi Inoue*[,†]

[†]Institut für Chemie, Technische Universität Berlin, Straße des 17. Juni 135, Sekr. C2, D-10623 Berlin, Germany

[‡]Department of Inorganic and Analytical Chemistry, Budapest University of Technology and Economics, Szent Gellért tér 4, 1111 Budapest, Hungary

Supporting Information

ABSTRACT: The reactivity of ylide-like phosphasilene **1** [LSi(TMS)═P(TMS), L = PhC(N*t*Bu)$_2$] with group 10 d^{10} transition metals is reported. For the first time, a reaction of a phosphasilene with a transition metal that actually involves the silicon−phosphorus double bond was found. In the reaction of **1** with ethylene bis(triphenylphosphine) platinum(0), a complete silicon−phosphorus bond breakage occurs, yielding the unprecedented dinuclear platinum complex **3** [LSi{Pt(PPh$_3$)}$_2$P(TMS)$_2$]. Spectroscopic, structural, and theoretical analysis of complex **3** revealed the cationic silylene (silyliumylidene) character of the silicon unit in complex **3**. Similarly, formation of the analogous dinuclear palladium complex **4** [LSi{Pd(PPh$_3$)}$_2$P(TMS)$_2$] from tetrakis(triphenylphosphine) palladium(0) was observed. On the other hand, in the case of bis(cyclooctadiene) nickel(0) as starting material, a distinctively different product, the bis(silylene) nickel complex **5** [{(LSi)$_2$P(TMS)}Ni(COD)], was obtained. Complex **5** was fully characterized including X-ray diffraction analysis. Density functional theory calculations of the reaction mechanisms showed that the migration of the TMS group in the case of platinum and palladium was induced by the oxidative addition of the transition metal into the silicon−silicon bond. The respective platinum intermediate **2** [LSi{Pt(TMS)(PPh$_3$)}P(TMS)] was also experimentally observed. This is contrasted by the reaction of nickel, in which the equilibrium of phosphasilene **1** and the phosphinosilylene **6** [LSiP(TMS)$_2$] was utilized for a better coordination of the silicon(II) moiety in comparison with phosphorus to the transition metal center.

INTRODUCTION

Compounds with silicon phosphorus double bonds, phosphasilenes, have found the attention of researchers since their polarized double bonds exhibit interesting electronic structures and reactivities.[1] In general, these compounds are synthetically challenging because of the pronounced polarity of the Si−P multiple bonds owing to the difference in electronegativity between Si and P atoms. Since the first phosphasilene, **I** (Chart 1), was described in 1984 by Bickelhaupt et al.,[2] several phosphasilenes could be synthesized and characterized.[3] Afterward, thorough investigations into the reactivity of phosphasilene **II** were reported by Driess et al. in 1996 (Chart 1).[3g] These reactivity investigations of phosphasilene **II** focus on small, organic molecules mainly featuring additions to the Si═P double bond, whereas the reactivity of phosphasilenes toward transition metals is to date still scarcely studied. To the best of our knowledge, the only two examples showed either a coordination of the lone pair on phosphorus to the transition metal (see **III** in Chart 1)[4] or a substitution of a hydrogen on phosphorus with methylzinc (see **IV** in Chart 1).[5] The silicon−phosphorus double bond itself was inert under these conditions. The reactivity of a phosphasilene naturally depends on the polarization of the double bond which is determined by the substituents on phosphorus and silicon in addition to the reactivity of the substituents themselves. The polarization of a Si═P double bond can be decreased or even reversed by choosing a combination of substituents with opposing electronic effects on the Si═P double bond, such as in phosphasilene **V**.[3i] Meanwhile, Driess and co-workers, very recently, reported the highly polarized phosphasilene **VI** and its remarkable application as a phosphinidene transfer reagent.[6] We recently reported the synthesis and isolation of zwitterionic phosphasilene **1** (Chart 1).[7] This phosphasilene (**1**) showed an enhanced polarization of the double bond that is higher than that in any previously reported phosphasilene.[2−5] The amidinato chelate ligand facilitates the positive partial charge on the unsaturated silicon atom, while the trimethylsilyl group on the phosphorus atom is stabilizing its negative partial charge. In this study, we focus on the reactivity of the ylide-like phosphasilene **1** toward group 10 d^{10} transition metals. We report on a reactivity that goes beyond the simple coordination of a lone pair on the phosphorus to the transition metal or a simple exchange of the substituent on phosphorus, but leads to a breakage of the silicon−phosphorus double bond. Moreover, the isolation and full characterization of the first neutral base-stabilized silyliumylidene-phosphide diplatinum complex[8] as well as a novel phosphorus-bridged bis(silylene) nickel complex is reported. In addition, the reaction mechanisms of their formations were investigated by density functional theory (DFT) calculations.

Received: September 24, 2013
Published: October 30, 2013

dx.doi.org/10.1021/ja409720c | J. Am. Chem. Soc. 2013, 135, 17958−17968

Chart 1. Examples of Relevant Phosphasilenes and Phosphasilene Transition Metal Complexes

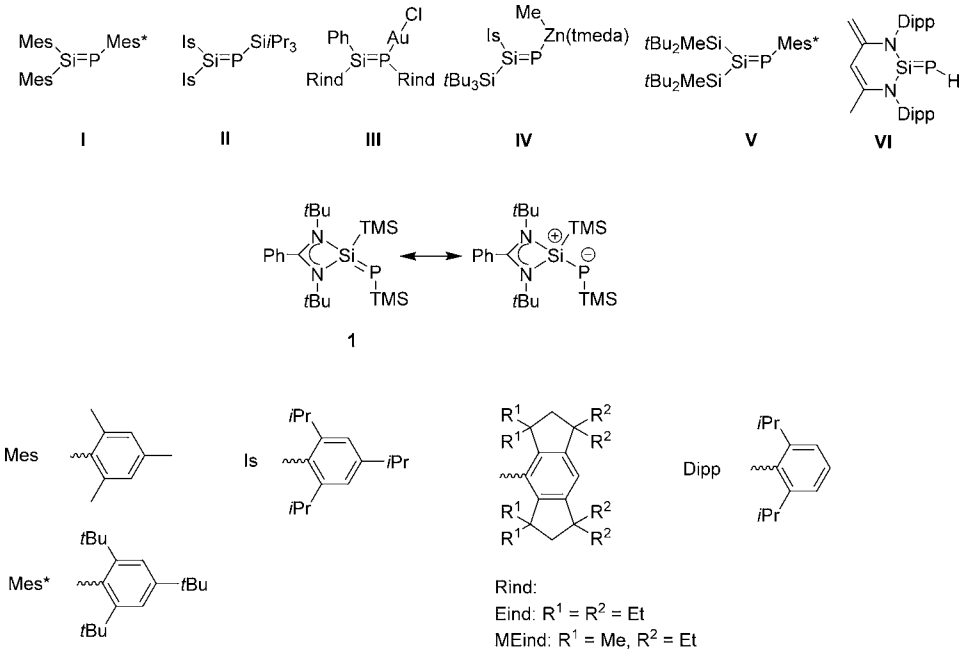

RESULTS

We chose the platinum(0) source ethylene bis(triphenylphosphine)platinum $[(\eta^2\text{-}C_2H_4)Pt(PPh_3)_2]$ as the starting point of our investigations into the reactivity of the zwitterionic phosphasilene **1** with group 10 d^{10} transition metals. When phosphasilene **1** was reacted with 1 molar equivalent of $[(\eta^2\text{-}C_2H_4)Pt(PPh_3)_2]$ at −30 °C, a brown-colored solution was obtained that consists after 1 h at low temperatures of the platinum complex **2** as the main product (Scheme 1). Complex **2**

Scheme 1. Reactivity of Phosphasilene 1 with $[(\eta^2\text{-}C_2H_4)Pt(PPh_3)_2]$ Giving Rise to the Intermediate Platinum Complex 2 and Finally the Dinuclear Platinum Complex 3

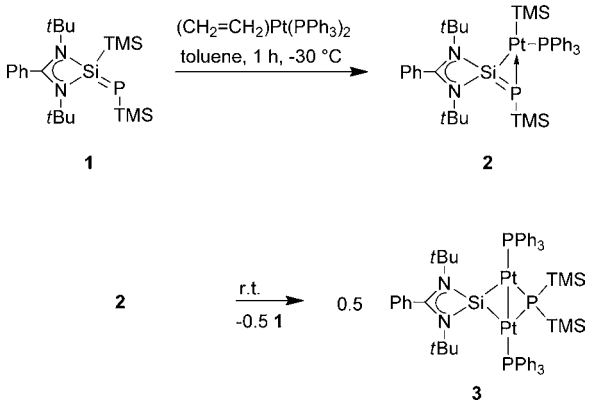

has been characterized based on ^1H, ^{31}P, and ^{195}Pt NMR spectroscopy. The migration of the trimethylsilyl (TMS) group from the central silicon atom to platinum can easily be seen in the ^1H NMR spectrum of **2**. The ^1H NMR spectrum of **2** exhibits in addition to the singlet for the *t*Bu groups (δ = 1.26 ppm) and the doublet for the TMS group on the phosphorus atom (δ = 0.42 ppm, $^3J_{P-H}$ = 4.0 Hz), one singlet with satellites for the TMS group on the platinum atom (δ = 0.61 ppm, $^3J_{Pt-H}$ = 32.8 Hz). This chemical shift and coupling constant fit well with those of other species consisting of platinum-bond trimethylsilyl groups (δ = 0.35−0.56 ppm, $^3J_{P-H}$ = 24.5−33.5 Hz).[9]

In the $^{31}P\{^1H\}$ NMR spectrum of **2**, two signals were observed at δ = 37.1 and −308.7 ppm. The doublet with satellites at 37.1 ppm ($^2J_{P-P}$ = 19.1 Hz) corresponds to the PPh_3 ligand. The coupling constant of PPh_3 with platinum in **2** ($^1J_{Pt-P}$ = 2453 Hz) is in the range of coupling constants of PPh_3 groups on a platinum(II) atom (1705−2558 Hz),[10] whereas the coupling constants for PPh_3 groups in platinum(0) complexes are 3232−4438 Hz.[11] The doublet with satellites at δ = −308.7 ppm belongs to the silene-bond phosphorus. The small coupling constant with platinum ($^1J_{Pt-P}$ = 358 Hz) is similar to those in side-on bonded diphosphine platinum complexes ($^1J_{Pt-P}$ = 52.1−255 Hz).[12] The $^{195}Pt\{^1H\}$ NMR spectrum of **2** exhibits one doublet of doublets of doublets at δ = 4653 ppm ($^1J_{Pt-P}$ = 2466 Hz, $^1J_{Pt-P}$ = 359 Hz). The coupling between platinum and the TMS protons was confirmed by ^{195}Pt spectroscopy ($^3J_{Pt-H}$ = 32.8 Hz). Moreover, the characterization of species **2** was confirmed by high-resolution mass spectrometry and an optimized structure of **2** was found by DFT calculation (vide infra, Figure 6).

In spite of our efforts, the reactive complex **2** could not be isolated. The generation of the new dinuclear platinum complex **3** and the concomitant formation of phosphasilene **1** from platinum complex **2** were observed (Scheme 1). This reaction is accelerated at ambient temperature. The synthesis of **3** was optimized by changing the ratio of the starting materials. Two molar equivalents of $[(\eta^2\text{-}C_2H_4)Pt(PPh_3)_2]$ were reacted with **1** at −30 °C, and the reaction mixture was slowly warmed up to room temperature for 3 h and stirred for 16 h to give the desired dinuclear platinum complex **3** as a single product. Analytically pure compound **3** was obtained in 52% yield by precipitation from a concentrated toluene solution through the addition of hexane.

The ^1H NMR spectrum of **3** displays one singlet for the *t*Bu groups (δ = 0.92 ppm) and one doublet for the trimethylsilyl moieties (δ = 0.46 ppm, $^3J_{P-H}$ = 5.2 Hz). The $^{31}P\{H\}$ NMR spectrum presents two signals at δ = 56.0 and −94.6 ppm, which correspond to the PPh_3 and $P(TMS)_2$ moieties, respectively

dx.doi.org/10.1021/ja409720c | J. Am. Chem. Soc. 2013, 135, 17958−17968

(Figure 1a). The upfield signal caused by the $P(TMS)_2$-phosphorus atom is a triplet ($^2J_{P-P}$ = 33.3 Hz) with three

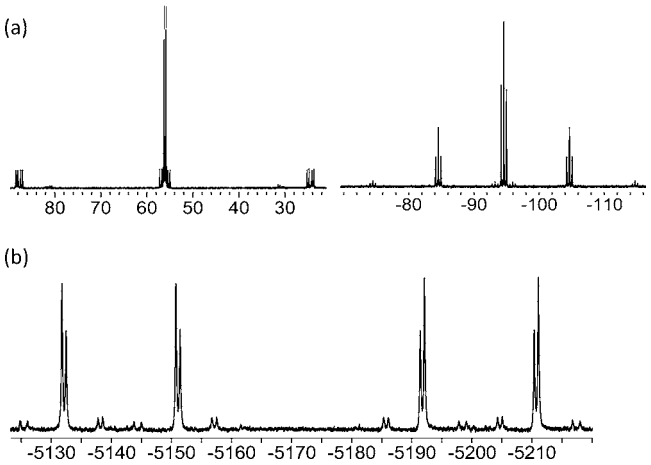

Figure 1. (a) $^{31}P\{^1H\}$ NMR spectrum and (b) $^{195}Pt\{^1H\}$ NMR spectrum of **3**.

satellites. The satellite with higher intensity originates from the coupling to platinum with one ^{195}Pt in the isotopomeric structure[13] ($I \approx 45\%$, $^1J_{P-Pt}$ = 1633 Hz), whereas the second satellite belongs to the isotopomer with two ^{195}Pt atoms ($I \approx 11\%$, $^1J_{P-Pt}$ = 1633 Hz). The last and less intense satellite corresponds to the coupling with the silicon atom bonded to both platinum atoms ($I \approx 5\%$, $^1J_{Si-P}$ = 219.2 Hz). Meanwhile, the analysis of the downfield signal (δ = 56.0 ppm) is more complex due to the magnetic inequivalency of the phosphorus atoms once the isotopomer with one ^{195}Pt is considered, turning the spin system AMX into AA′MM′X. The main signal shows a doublet ($^2J_{P-P}$ = 33.3 Hz), while the satellites show a doublet of doublets. The satellite for the PPh_3 in direct vicinity of the ^{195}Pt ($^1J_{Pt-P}$ = 5137 Hz) shows a large coupling between the two PPh_3 groups ($^3J_{P-P}$ = 86.4 Hz). This coupling is also observed in the second satellite ($^2J_{Pt-P}$ = 60.5 Hz) overlapping with the main signal. These couplings are confirmed by $^{195}Pt\{^1H\}$ NMR spectroscopy (Figure 1b), where a doublet of doublets was obtained with the same values for $^1J_{Pt-P}$ and $^2J_{Pt-P}$. In this spectrum, small satellites are visible in each doublet corresponding to the coupling $^1J_{Pt-Si}$ of 1117.0 Hz.

Comparing the high coupling constant of $^1J_{Pt-P}$ = 5137 Hz in **3** with known triphenylphosphine diplatinum complexes (with a Pt−Pt bond, $^1J_{Pt-P}$ = 3849−5468 Hz;[14] without a Pt−Pt bond, $^1J_{Pt-P}$ = 1458−2394 Hz[15]), the structure of **3** is likely to present a Pt−Pt bond. The $^3J_{P-P}$ in diplatinum complexes with Pt−Pt bond are around 55−81 Hz,[14] whereas in complexes with no Pt−Pt bond, this coupling is absent[15c] or its coupling constant has a very low value ($^3J_{P-P}$ = 18−29 Hz).[15a,b] The chemical shift of the signal in the $^{195}Pt\{H\}$ NMR spectrum of −5172 ppm is in the same range as those of two known diplatinum complexes (δ = −5570 and −5835 ppm).[14b,d] Regarding the $^{29}Si\{H\}$ NMR, two signals are observed (δ = 8.3 and 234.5 ppm). The upfield signal, a doublet ($^2J_{P-Si}$ = 7.4 Hz), is related to the silicon atoms of the TMS groups, and the downfield signal belongs to the bridging silyliumylidene moiety. The chemical shift of the latter is considerably downfield shifted from those of known N-heterocyclic silylene transition metal complexes.[16] It has the expected shape of a doublet of triplets ($^2J_{Si-P(TMS)_2}$ = 219.4 Hz, $^2J_{Si-PPh_3}$ = 48.5 Hz).

Crystals of **3** suitable for single crystal X-ray diffraction analysis were grown from benzene, and thus, the molecular structure of **3** was determined (Figure 2). The silyliumylidene moiety and the

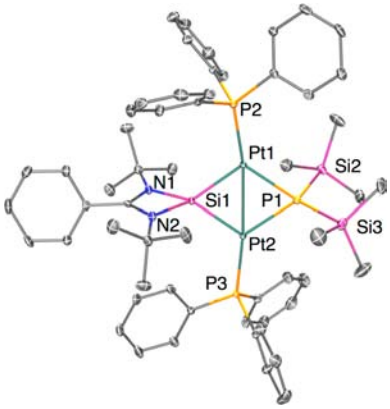

Figure 2. Molecular structure of **3**. Thermal ellipsoids are drawn at the 50% probability level. Hydrogen atoms and one molecule of benzene are omitted for clarity. Selected bond lengths [Å] and angles [deg]: Pt1−Pt2 2.6466(5), Pt1−Si1 2.274(2), Pt2−Si1 2.285(2), Pt1−P1 2.360(2), Pt2−P1 2.367(2), Pt1−Si1−Pt2 70.98(5), Pt1−P1−Pt2 68.09(4), Si1−Pt1−P1 110.78(6), Si1−Pt2−P1 110.15(6), P2−Pt1−Pt2 173.63(4), P3−Pt2−Pt1 170.92(4), P1−Pt1−Pt2−Si1 179.60(7).

phosphide group are coordinated to two platinum atoms with Pt1−Si1−Pt2 and Pt1−P1−Pt2 angles of 70.98(5)° and 68.09(4)°, respectively. The Pt−Si−Pt angle in **3** is almost identical to the angles of dinuclear bis(silyl) platinum complexes with Pt−Pt bond (69.3(2)−71.8(2)°)[14a−c] and much smaller than those of dinuclear bis(silyl) platinum complexes without Pt−Pt bond (99.4(2)−112.51(3)°).[15a,b,17] The Si−Pt−P angles in **3** (110.78(6)° and 110.15(6)°) are similar to the Si−Pt−Si angles of the dinuclear bis(silyl) platinum complexes with Pt−Pt bond (109.4(2)−110.4(2)°)[14a−c] rather than to the P−Pt−P angles in a dinuclear platinum bisphosphino complex with Pt−Pt bond (122.17(5)° and 127.53(5)°).[14d] The triphenylphosphine ligands in **3** are coordinated on the Pt atom like a slightly tilted elongation of the Pt−Pt bond (P−Pt−Pt 173.63(4)° and 170.92(4)°) similarly to other P−Pt−Pt coordinations in dinuclear platinum complexes with Pt−Pt bond (161.4(2)−177.45(4)°).[14] The P1−Pt1−Pt2−Si1 torsion angle of **3** (179.60(7)°) illustrates that the Pt_2SiP plane is almost planar.

The Pt−Pt bond length of **3** (2.6466(5) Å) is in the range of the respective lengths in dinuclear platinum complexes with Pt−Pt bond (2.604(1)−2.7032(6) Å).[14,15c] This fact attests the existence of a Pt−Pt bond in **3**. The Pt−Si bond lengths in **3** (2.274(2) and 2.285(2) Å) are close to those in a cationic silylene platinum complex (2.270(2)−2.388(3) Å),[18] but longer than those in neutral platinum silylene complexes (2.2076(15)−2.210(2) Å).[19] This bonding nature was also studied by DFT calculation (vide infra).

The molecular orbitals of the dinuclear platinum complex **3** were calculated at the B3PW91/6-31G(d)/LANL2DZ [Pt] level of theory to describe the bonding situation at platinum (Figure 3). The HOMO of compound **3** supports bonding interactions between the lone pair orbital of the silyliumylidene moiety and the lone pair orbital of the phosphide with the empty d-orbitals of the platinum atoms. The HOMO-1 describes π-type interactions between the d-orbital on platinum with the vacant p-orbital on the silicon atom and the p-type lone pair on the phosphide. The

dx.doi.org/10.1021/ja409720c | J. Am. Chem. Soc. 2013, 135, 17958−17968

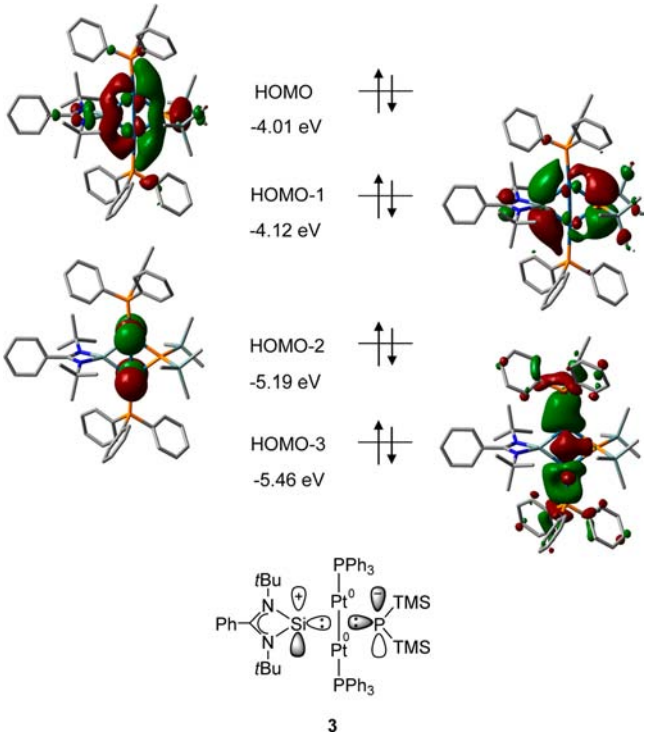

Figure 3. Molecular orbitals for the dinuclear platinum species **3** calculated at the B3PW91/6-31G(d)/LANL2DZ [Pt] level of theory and schematic representation of the bonding situation in **3** according to the MOs.

HOMO-3 confirms the platinum−platinum bond. The schematic representation of this situation is shown as **3** in Figure 3.

DFT studies were also utilized to discriminate between the two possible resonance structures shown in Figure 4. Resonance

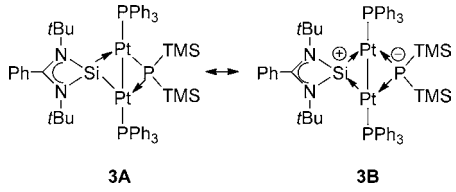

Figure 4. Two possible resonance structures of **3**, **3A** and **3B**, of which **3B** is indicated to be the more dominant one according to DFT calculations.

structure **3A** describes a platinum(I) species with each one covalent bond and one dative bond between platinum and phosphorus and silicon, while resonance structure **3B** depicts a platinum complex with only donating interactions between platinum and a cationic silicon(II) (silyliumylidene) unit and an anionic phosphide group. The calculated NBO charge in **3** (+0.974 on silicon and −0.715 on phosphorus) reveals a charge separated resonance structure of **3** and thus points to the domination of **3B** over **3A**. In addition, the NBO charge of an uncoordinated free LSi^+ fragment and the cationic silicon(II) platinum complex LSi^+PtPPh_3 on silicon atom amounts to +1.337 and +1.219, respectively. These results show that a relatively large amount of the positive charge on silicon atom is still present in **3** despite its coordination to the diplatinum moiety, supporting the resonance structure **3B**. The WBI (Wiberg bond indices) values were calculated for silicon−platinum to be 0.7606 and 0.7504, for phosphorus−platinum to be 0.4407 and 0.4448, and for platinum−platinum to be 0.2799. This fits well with the assignment to resonance structure **3B**. Although silyliumylidene cations are rare species, few stable silyliumylidene cations were reported.[20] In fact, silyliumylidene cations stabilized by the amidinate ligand were only postulated reactive intermediates[21] or isolated as a 4-dimethylaminopyridine adduct[22] so far.

Moving up one row in the periodic table, phosphasilene **1** was reacted with one and two molar equivalents of tetrakis(triphenylphosphine)palladium(0), $[Pd(PPh_3)_4]$. In contrast to the reaction with the platinum(0) complex $[(\eta^2\text{-}C_2H_4)Pt(PPh_3)_2]$, no reaction between **1** and $[Pd(PPh_3)_4]$ was observed by ^1H NMR spectroscopy at low temperatures and ambient temperature. Slightly elevated temperatures of 40−50 °C were required for the formation of the dinuclear palladium species **4**, while no intermediate related to **2** could be observed (Scheme 2).

Scheme 2. Synthesis of the Dinuclear Palladium Complex 4

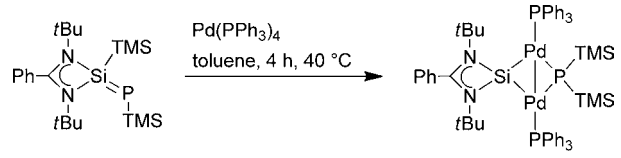

Complex **4** was characterized based on ^1H, ^{13}C, ^{29}Si, and ^{31}P NMR spectroscopy and high resolution mass spectrometry. The ^1H NMR of complex **4** resembles the one of complex **3** described above. It reveals one doublet for two identical TMS groups coupling to phosphorus at δ = 0.54 ppm ($^3J_{H-P}$ = 5.2 Hz) and a singlet for the *tert*-butyl groups at δ = 0.86 ppm. Similarly, the $^{31}P\{^1H\}$ NMR spectrum of complex **4** with a doublet at δ = 41.2 ppm ($^2J_{P-P}$ = 11.2 Hz) for the triphenylphosphine group and a triplet at δ = −163.4 ppm ($^2J_{P-P}$ = 11.2 Hz) is a simplification of the respective spectrum of complex **3** [56.0 ppm, ($^2J_{P-P}$ = 33.3 Hz, $P(Ph)_3$), −94.6 ppm ($^2J_{P-P}$ = 33.3 Hz, $P(TMS)_2$], since palladium unlike platinum is not NMR active. The resonance of the $P(TMS)_2$ show that these phosphorus atoms are significantly more shielded in the palladium complex **4** than in the platinum complex **3**.

$^{29}Si\{^1H\}$ NMR spectroscopy attests to the low-valent silicon atom with a chemical shift of 187.8 ppm. This is significantly downfield shifted compared to dipalladium complexes with bridging silylene or silyl groups (δ = 109.5 and 126 ppm, respectively).[23] A comparison with the chemical shift of the silylene in the dinuclear platinum species **3** (δ = 234.5 ppm) reveals an upfield shift of the silylene unit in the dinuclear palladium species **4** (δ = 187.8 ppm). For comparable silylene-bridged dinuclear palladium and platinum complexes, a similar trend was observed (δ = 109.5 and 188.1 ppm, respectively).[23a,14b] This doublet of triplets exhibits the coupling of the silyliumylidene-silicon with the two equivalent triphenylphosphine groups ($^2J_{Si-PPh_3}$ = 43.3 Hz) and the bis(trimethylsilyl)-phosphide ($^2J_{Si-PTMS_2}$ = 184.3 Hz), which is comparable to, but lower than the respective coupling constants in **3** ($^2J_{P-Si}$ = 219.2 Hz, 48.5 Hz). The signal for the TMS-silicon appears as a doublet at δ = 0.01 ppm ($^1J_{P-Si}$ = 6.0 Hz).

Ascending the group 10 to the top, phosphasilene **1** was reacted with $[Ni(PPh_3)_4]$ in toluene. However, neither at low temperature, room temperature nor at slightly elevated temperatures of 50 °C any reaction was observed, while more intense

dx.doi.org/10.1021/ja409720c | J. Am. Chem. Soc. 2013, 135, 17958−17968

Scheme 3. Reaction of Phosphasilene 1 and the Phosphinosilylene 6 with $Ni(COD)_2$ Yielding the Bis(silylene) Nickel Complex 5 and $P(TMS)_3$

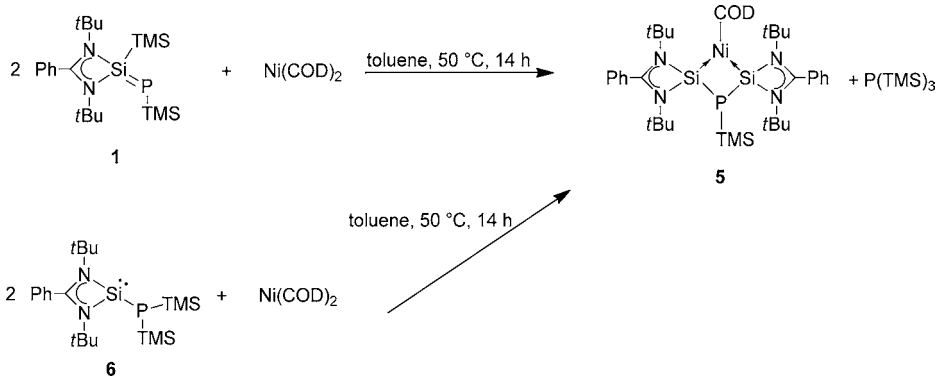

heating to 90 °C destroyed the nickel starting material. Circumventing this problem, we chose the common nickel(0) source bis(1,5-cyclooctadiene)nickel, $[Ni(COD)_2]$, as a starting material. The reaction of phosphasilene **1** with one molar equivalent of $[Ni(COD)_2]$ did not proceed at low or ambient temperatures. Elevated temperatures of 50 °C were required for the conversion of the starting materials. ^1H NMR spectroscopy revealed that the formed product, **5**, is significantly different from **2**, **3**, and **4** (Scheme 3). The ^1H NMR spectrum of **5** exhibits one singlet for the *t*Bu groups (δ = 1.41 ppm) and one doublet for the TMS group on phosphorus (δ = 0.57 ppm, $^3J_{P-H}$ = 4.4 Hz). According to the intensity ratios of the signals for the *t*Bu groups and the TMS group, it was predicted that **5** contains two silylene units and one phosphine-bond TMS group. Broad peaks for the COD ligand were also observed, indicating that one COD is coordinated to the nickel atom. $^{31}P\{^1H\}$ NMR spectroscopy reinforces this assignment as one singlet with silicon satellites is observed at δ = −125.4 ppm ($^1J_{Si-P}$ = 73.7 Hz) for **5**. In the ^1H and $^{31}P\{^1H\}$ NMR spectra of a crude sample, one doublet (^1H NMR: δ = 0.30 ppm, $^3J_{P-H}$ = 4.4 Hz) and one singlet (^{31}P NMR: δ = −252.3 ppm) corresponding to $P(TMS)_3$ are clearly observed in addition to the signals for **5**.[24] The ^{29}Si NMR spectra of **5** exhibit one doublet for the silicon(II) atom at δ = 51.5 ppm ($^1J_{P-Si}$ = 73.2 Hz) and one doublet for the trimethylsilyl group at δ = −9.2 ppm ($^1J_{P-Si}$ = 75.8 Hz). The observed chemical shift for the ^{29}Si(II) nuclei in **5** (51.5 ppm) is downfield of the chemical shift of the ^{29}Si(II) nuclei in a previously reported oxygen-bridged bis(silylene) nickel complex $[\{(LSi)_2O\}Ni(COD)]$ (δ = 32.8 ppm).[25]

Usage of 0.5 molar equivalents of $[Ni(COD)_2]$ resulted in an incomplete reaction. The phosphasilene **1** was found to be still present in the reaction mixture to approximately 30% by ^1H NMR spectroscopy. This is presumably due to the instability of $[Ni(COD)_2]$ at the reaction temperature. Therefore, the reaction conditions were optimized using 0.67 molar equivalents of $[Ni(COD)_2]$. Crystallization of the crude product from a concentrated toluene solution at −30 °C afforded dark red crystals of the bis(silylene) nickel complex **5** in 73% yield (Scheme 3). Considering the reaction mechanism for the formation of **5**, we probed the reactivity of the related phosphinosilylene **6**[7] $[LSiP(TMS)_2]$ with half an equivalent of $[Ni(COD)_2]$, which similarly lead to the formation of the bis(silylene) nickel complex **5** as the main product (Scheme 3).

The molecular structure of **5** was unambiguously determined by single crystal X-ray diffraction analysis as displayed in Figure 5.[26] The phosphine-bridged two silicon(II) subunits and one

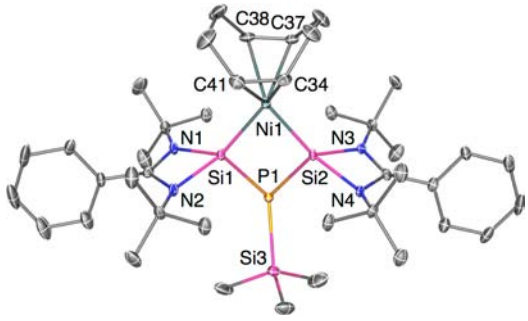

Figure 5. Molecular structure of **5**. Thermal ellipsoids are drawn at the 50% probability level. Hydrogen atoms and two molecules of toluene are omitted for clarity. Selected bond lengths [Å] and angles [deg]: Ni1−Si1 2.201(2), Ni−Si2 2.202(1), Si1−P1 2.250(2), Si2−P1 2.263(2), Si1−Ni1−Si2 79.80(6), Si1−P1−Si2 77.49(7), Ni1−Si1−Si2−P1 165.31(9).

COD ligand are coordinated to the nickel atom with a Si1−Ni1−Si2 angle of 79.80(6)°, which is larger than the Si−Ni−Si angle of the related oxygen-bridged bis(silylene) nickel complex $[\{(LSi)_2O\}Ni(COD)]$ (68.90(3)°).[25] However, the Si1−P1−Si2 angle in **5** (77.49(7)°) is smaller than the Si−O−Si angle in $[\{(LSi)_2O\}Ni(COD)]$ (93.44(8)°). This geometrical torsion causes a distorted Ni1−Si1−P1−Si2 plane in **5** (the P atom deviates by 14.65° from the Si1−Ni1−Si2 plane, torsion angle Ni1−Si1−Si2−P1 165.31(9)°), while the Ni−Si−O−Si plane of $[\{(LSi)_2O\}Ni(COD)]$ is almost planar (Ni−Si−O−Si 179.76(9)°).[25] The Ni−Si bond lengths in **5** (2.201(2) Å and 2.202(1) Å) are slightly longer than those found in $[\{(LSi)_2O\}$-Ni(COD)] (2.1908(7) Å and 2.1969(7) Å),[25] but slightly shorter than those in the bis(silylene) nickel complex $[\{(CHNtBu)_2Si\}_2Ni(CO)_2]$ (2.207(2) Å and 2.216(2) Å).[27] Moreover, the Ni−Si bond lengths in **5** are significantly longer than that in the ylide-like silylene nickel complexes $[(\{DippNC(CH_2)CHC(Me)NDipp\}Si)$-$Ni(C_6H_6/C_7H_8)]$ (2.0597(10) Å and 2.0647(6) Å).[28]

DFT calculations at the B97-D/cc-pVTZ/(SMD=toluene)//B97-D/6-31G* level of theory (cc-pVTZ-PP on Pt and Pd atoms and cc-pVTZ on Ni atoms) were carried out to better understand the formation of the final products **3**−**5** and to gain insights into the different reactivity of phosphasilene **1** with platinum, palladium, and nickel (Figures 6−8). Mechanistic investigations for the formation of the dinuclear platinum complex **3** revealed the rate determining step to be the dissociation of a triphenylphosphine group from the platinum(0) starting ma-

dx.doi.org/10.1021/ja409720c | J. Am. Chem. Soc. 2013, 135, 17958−17968

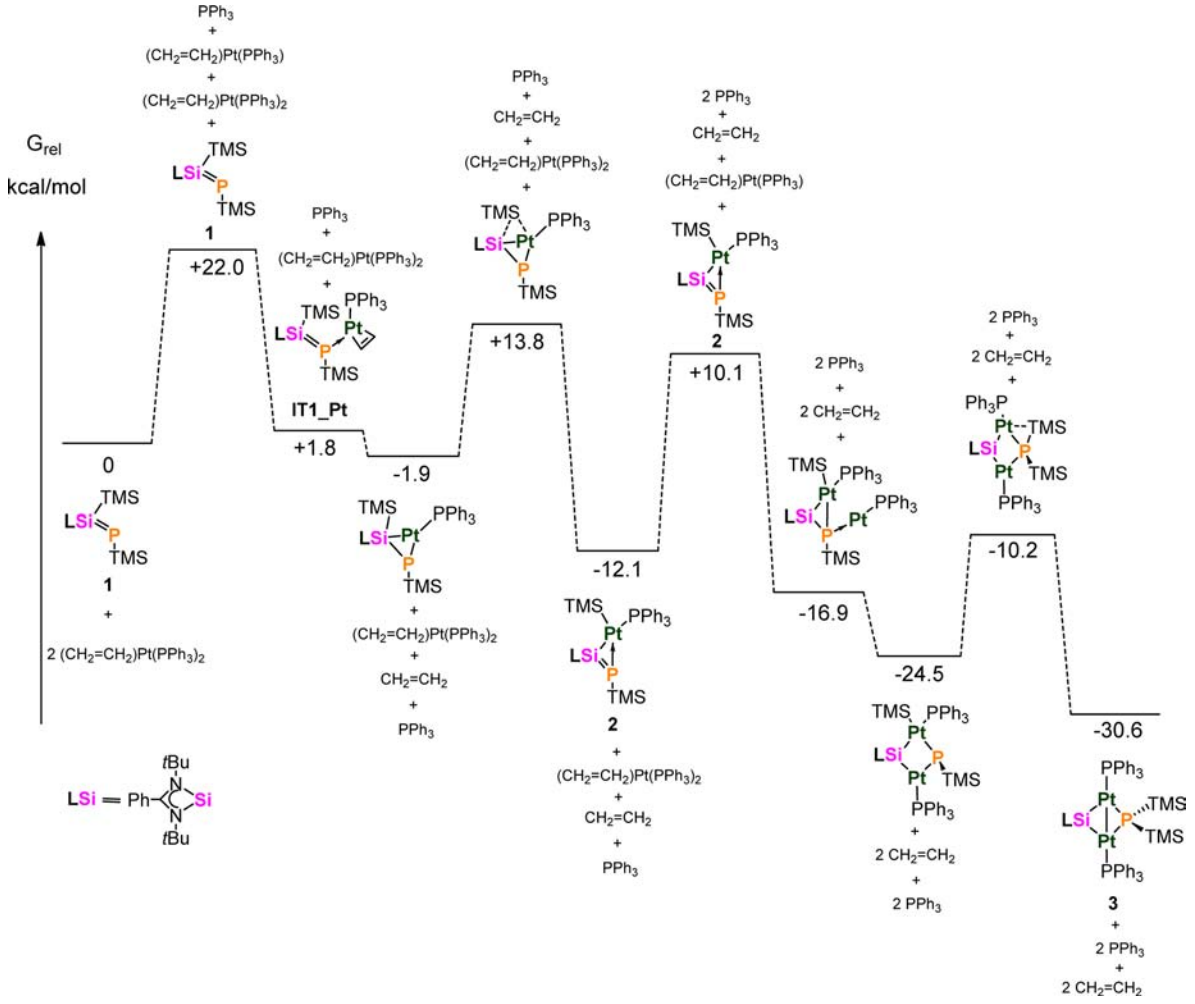

Figure 6. Results of DFT calculation at the B97-D/cc-pVTZ/(SMD = toluene)//B97-D/6-31G* level of theory (cc-pVTZ-PP on Pt atoms) of the simplified mechanisms for the formation of **3** (for the detailed mechanism, please see the Supporting Information, Scheme S1).

terial with a feasible energy of +22.0 kcal/mol (Figure 6). The coordination of the phosphorus of a phosphasilene to a transition metal was previously reported in the phosphasilene gold complex **III** (Chart 1).[4] The respective intermediate in this platinum mechanism, **IT1_Pt**, is succeeded by an addition of the platinum center to the phosphorus−silicon double bond and the insertion of the platinum atom into the silicon−silicon bond. Complex **2** was found to be quite stable, −12.1 kcal/mol, and a considerably high activation barrier for the next step, the dissociation of another PPh_3 from the platinum starting material, was determined. This agrees well with the experimental observation of species **2**. The coordination of the phosphasilene-phosphorus atom to the second platinum is followed by rearrangements leading to the complete breakage of the silicon−phosphorus double bond, while both, silicon and phosphorus get bond to each of the platinum centers. The final step is a migration of the TMS group on platinum to phosphorus yielding the remarkably stable product **3** (−30.6 kcal/mol).

Elucidation of the mechanism for the formation of the palladium analogue, **4**, revealed as one major difference to the formation of diplatinum complex **3**, the higher activation barrier for the formation of the reactive palladium species $Pd(PPh_3)$ with +28.7 kcal/mol (+22.0 kcal/mol for Pt) (Figure 7). This was also experimentally observed by the required elevated temperatures in the reaction with palladium, whereas the initial steps of the platinum reaction yielding **2** occurred at −30 °C. The palladium analogue to species **2** [**2_Pd**] is considerably less stable (+0.9 kcal/mol compared to −12.1 kcal/mol in **2**). The subsequent intermediates of **2_Pd** with energies lower than those in the platinum mechanism as well as the elevated temperatures in the palladium reaction can explain that it was impossible to observe complex **2_Pd** experimentally. Another interesting difference in the mechanisms for palladium and platinum is the migration of the TMS group from the transition metal to the phosphorus atom. In the case of palladium, this occurs before the income of another $Pd(PPh_3)$ moiety. Complex **IT2_Pd** [$(PPh_3)PdSiP(TMS)_2$] is even more stable than complex **2_Pd** (−3.3 kcal/mol compared to +0.9 kcal/mol). A respective platinum species was also computationally found (see Supporting Information, Scheme S2). However, the intermediates on the mechanism shown in Figure 6 have lower energies.

Based on the different product obtained with nickel, the approach for the mechanistic DFT investigations was altered. Considering the bis(silylene) nickel product, a reasonable intermediate in this mechanism is a nickel complex with one phosphinosilylene **6** being coordinated (**IT2_Ni**, Figure 8). Indeed, phosphinosilylene nickel complex **IT2_Ni** was found to be stable with +1.3 kcal/mol. Three pathways were considered for the formation of **IT2_Ni**: (i) the oxidative addition of nickel into the silicon−silicon bond (similar to the platinum and

dx.doi.org/10.1021/ja409720c | J. Am. Chem. Soc. 2013, 135, 17958−17968

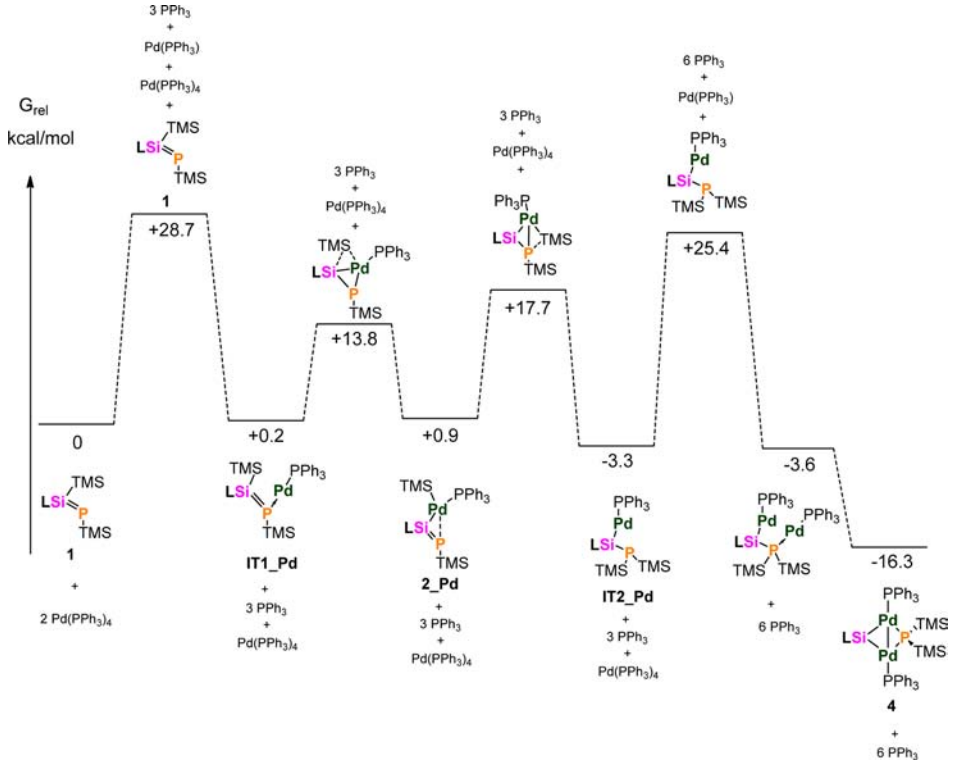

Figure 7. Results of DFT calculation at the B97-D/cc-pVTZ/(SMD = toluene)//B97-D/6-31G* level of theory (cc-pVTZ-PP on Pd atoms) of the simplified mechanisms for the formation of **4** (for the detailed mechanism, please see the Supporting Information, Scheme S3).

palladium reactions), (ii) the TMS migration being activated by the coordination of phosphasilene **1** to the nickel center, and (iii) the TMS migration independent of the presence of nickel. These DFT calculations showed that the isomerization of the phosphasilene **1** to the slightly less stable phosphinosilylene **6** (+1.9 kcal/mol) occurs before its coordination to the nickel center (compare the red and black pathways in the Supporting Information Scheme S4). The transition state **TS2_Ni** between the phosphasilene nickel complex, **IT1_Ni** (+9.9 kcal/mol), and the phosphinosilylene nickel complex, **IT2_Ni**, has a considerably high energy of +40.6 kcal/mol (Scheme S4). The barrier for the isomerization from the phosphasilene **1** into the phosphinosilylene **6**, **TS1_Ni**, without the influence of nickel is significantly lower (+32.1 kcal/mol). Also the highest activation energy in this black pathway, the loss of one COD ligand (+33.5 kcal/mol), is more feasible. No intermediate based on an oxidative addition of the nickel center into the silicon−silicon bond could computationally be found. Adjacent to the formation of another phosphinosilylene **6** from phosphasilene **1**, the coordination of its phosphorus to the silylene-coordinated nickel center was found, **IT3_Ni** (+4.1 kcal/mol). The concerted mechanism for the rearrangement of the TMS-group to form $P(TMS)_3$ has a transition state **TS3_Ni** of +31.9 kcal/mol. The found relatively high barriers, compared to the Pt reaction, are in accordance with the necessity of the experimentally observed elevated temperature. The generation of final products **5**, $P(TMS)_3$, and COD is giving a net energy gain of +15.1 kcal/mol. The activation of the TMS group on the phosphasilene silicon by the metal center lowering the barrier of the TMS migration appears to be not available for nickel because of the large steric demand of the COD ligand the nickel center cannot take part in the process.

Considering the different outcome of the reactions of phosphasilene **1** with platinum and palladium yielding the dinuclear metal complexes **3** and **4**, while its reaction with nickel produced the bis(silylene) complex **5**, we wanted to find out if the respective other products, a dinuclear nickel complex as well as platinum and palladium bis(silylene) complexes, would also be thermodynamically favored. The energies of the dinuclear nickel complex **Ni_2_COD** $[LSi\{Ni(COD)\}_2P(TMS)]$ was found to be −8.1 kcal/mol (Figure 9), while the bis(silylene) platinum and palladium complexes **LSi_2M_PPh_3** $[\{(LSi)_2P(TMS)\}M(PPh_3)_n]$ (M = Pt, Pd; n = 1, 2) were calculated to be more stable with two PPh_3 groups than with one (M = Pt; n = 1: −15.8 kcal/mol; M = Pt, n = 2: −20.9 kcal/mol; M = Pd, n = 1: −7.8 kcal/mol; M = Pd, n = 2: −12.1 kcal/mol). The formation of all unobserved compounds is thus also thermodynamically preferred, but in each case the obtained products are more thermodynamically stable (Ni: −8.1 vs −15.1 kcal/mol in **5**; Pt: −20.9 vs −30.6 kcal/mol in **3**; Pd: −12.1 vs −16.3 kcal/mol in **4**). Moreover, calculations showed that in the case of tetrakis(triphenylphosphine)nickel(0) $[Ni(PPh_3)_4]$ the thermodynamically favored product would be $[LSi\{Ni(PPh_3)\}_2P(TMS)_2]$ over $[\{(LSi)_2P(TMS)\}Ni(PPh_3)]$ (−17.4 and −5.5 kcal/mol, respectively). This indicates that the different ligand on nickel, COD, instead of PPh_3 is one of the main reasons for the formation of the different product. However, additional calculations showed that the activation barrier for a reaction with $Ni(PPh_3)_4$, the dissociation of three PPh_3 groups, is with +39.3 kcal/mol too high to be feasible at reaction temperatures that are suitable for the reaction.

SUMMARY AND CONCLUSIONS

We investigated the reactivity of the zwitterionic phosphasilene **1** with group 10 d^{10} transition metals. In contrast to previous

dx.doi.org/10.1021/ja409720c | J. Am. Chem. Soc. 2013, 135, 17958−17968

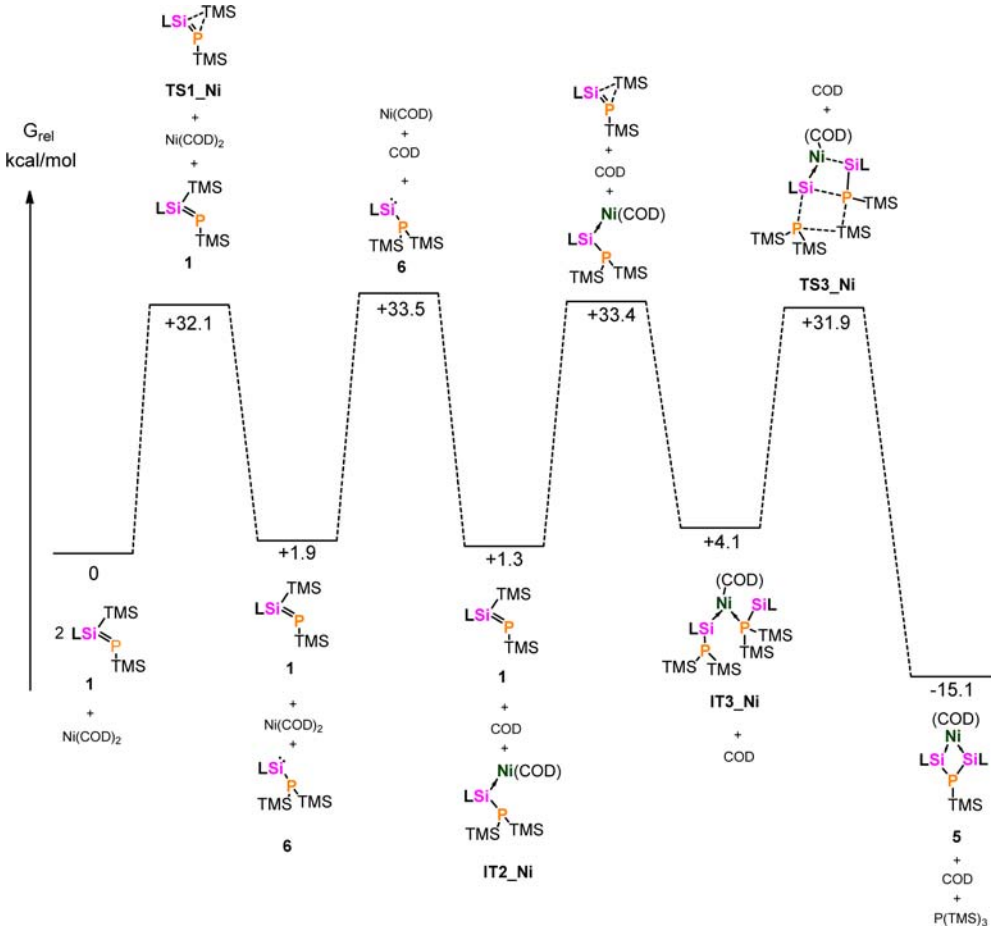

Figure 8. Results of DFT calculation at B97-D/cc-pVTZ/(SMD = toluene)//B97-D/6-31G* level of theory (cc-pVTZ on Ni atoms) of the mechanisms for the formation of **5**.

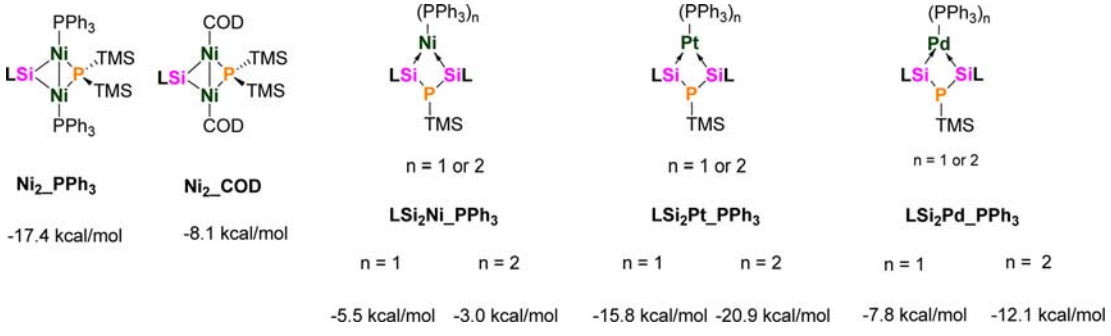

Figure 9. Results of DFT calculation at the B97-D/cc-pVTZ/(SMD = toluene)//B97-D/6-31G* level of theory (cc-pVTZ-PP on Pt and Pd atoms and cc-pVTZ on Ni atoms) of the energy for the unobserved species $[LSi\{Ni(PPh_3)\}_2P(TMS)_2]$, $[LSi\{Ni(COD)\}_2P(TMS)_2]$, and $[\{(LSi)_2P(TMS)\}M(PPh_3)_n]$ (M = Ni, Pt, Pd; n = 1, 2).

studies in which only a reaction on or coordination of the phosphine was reported,[4,5] we found a significantly different reactivity in which the phosphorus−silicon double bond takes part. In addition to the high polarization of the double bond, the presence of TMS groups is a key factor in the formation of the unexpected transition metal complexes. The TMS group was removed in all cases from the phosphasilene-silicon. We observed experimentally and supported by DFT calculations that the reaction between phosphasilene **1** and $[(\eta^2\text{-}C_2H_4)Pt(PPh_3)_2]$ proceeds via an oxidative addition of platinum into the silicon−silicon bond affording intermediate **2**. This reaction resulted in the formation of the unprecedented dinuclear platinum complex **3**, in which the platinum-bonded silicon is best described as a silyliumylidene. In the case of nickel, a different reactivity was found, affording a new chelating bis(silylene) ligand coordinated to the nickel center.

DFT calculations support that, in all cases, in reactions of the phosphasilene **1** with platinum, palladium, and nickel complexes, the TMS is shifted and removed from the phosphasilene-silicon atom to afford the coordination of the stronger silylene donor to the metal center. In the case of nickel, the isomerization of the phosphasilene to the phosphinosilylene occurred prior to its coordination to the metal center, whereas platinum and palladium were actively supporting the TMS migration as the

dx.doi.org/10.1021/ja409720c | J. Am. Chem. Soc. 2013, 135, 17958−17968

metal centers insert into the silicon−silicon bond. In all cases, the thermodynamically favored products (dinuclear metal complexes versus bis(silylene) metal complexes) were formed, suggesting that these are equilibrium reactions. Based on that, the ligand on nickel being COD instead of PPh_3, which is responsible for the thermodynamic stability of the products, would be a key factor for the different outcome of the reactions. These remarkable results could lead to a new class of transition metal complexes by taking advantage of the reactive zwitterionic phosphasilene **1** as a promising ligand. Reactivity studies of phosphasilene **1** with other transition metals as well as organic small molecules will be reported in due course.

EXPERIMENTAL SECTION

General Procedures. All experiments and manipulations were carried out under dry oxygen-free atmosphere using standard Schlenk techniques or in an MBraun inert atmosphere drybox containing an atmosphere of purified nitrogen. Solvents were dried using an M Braun purification system and stored over 3 Å molecular sieves. Ethylene bis(triphenylphosphine) platinum(0) (Aldrich), tetrakis-(triphenylphosphine) palladium(0) (STREM, 98%), and bis-(cyclooctadiene) nickel(0) (Aldrich, 99%) were used as received. The starting materials, phosphasilene **1** and phosphinosilylene **6**, were prepared according to the literature.[7] The deuterated solvents were degassed by freeze−pump−thaw technique and stored over 3 Å molecular sieves. The ^{1}H, $^{13}C\{^{1}H\}$, $^{29}Si\{^{1}H\}$, $^{31}P\{^{1}H\}$, ^{195}Pt, and $^{195}Pt\{^{1}H\}$ NMR spectra were recorded on Bruker Avance II 200 MHz, 400 MHz and Bruker Avance III 500 MHz Spectrometers. ^{1}H chemical shifts were referenced to the residual protons of C_6D_6 at 7.15 ppm or of THF-d_8 at 3.58 ppm, and ^{13}C chemical shifts were referenced to the carbon atoms of C_6D_6 at 128.00 ppm or THF-d_8 at 67.57 ppm. The $^{29}Si\{^{1}H\}$ NMR spectra were referenced to tetramethylsilane as an external standard, $^{31}P\{^{1}H\}$ spectra were externally calibrated with H_3PO_4 in sealed capillaries, and ^{195}Pt NMR spectra were calibrated to $K_2[PtCl_4]$ as an external standard. Melting points were determined from vacuum sealed capillaries on an electronic "Melting point tester" device from BSGT company and are uncorrected. For this purpose, samples were sealed off in capillaries under vacuum and heated slowly to observed decomposition or melting. High resolution APCI mass spectra were recorded on an Orbitrap LTQ XL of Thermo Scientific mass spectrometer. Elemental analysis was conducted on a Thermo Finnigan Flash EA 1112 series instrument.

Single-Crystal X-ray Structure Determinations. Crystals were mounted on a glass capillary in perfluorinated oil and measured in a cold N_2 flow. The data of compounds **3** and **5** was collected on an Oxford Diffraction Xcalibur S Sapphire at 150 K (Mo Kα radiation, λ = 0.71073 Å). The structures were solved by direct methods and refined on F2 with the SHELX-97 software package.[29] The positions of the H atoms were calculated and considered isotropically according to a riding model.

Preparation of [LSi{Pt(TMS)(PPh$_3$)}P(TMS)], 2. A toluene solution (5 mL) of (η^2-C_2H_4)Pt(PPh_3)$_2$ (201 mg, 0.269 mmol) was added to a solution of **1** (117 mg, 0.268 mmol) in toluene (10 mL) at −30 °C. The solution turned to a brown color and was stirred for 1 h at −30 °C. ^{1}H NMR (200.13 MHz, C_6D_6, 298 K): δ = 0.42 (d, 9 H, $^{3}J_{P-H}$ = 4.4 Hz, P(*TMS*)), 0.61 (s with satellite, 9 H, $^{3}J_{Pt-H}$ = 32.8 Hz, Pt(*TMS*)), 1.26 (s, 18 H, C*Me*$_3$), 6.95−7.00 (m, 5 H, C*Ph*), 7.44 (br, 9 H, P*Ph*$_3$), 8.01 (m, 6 H, *o*-P*Ph*$_3$) ppm. $^{31}P\{^{1}H\}$ NMR (161.976 MHz, C_6D_6, 298 K): δ = −308.7 (d with satellite, $^{1}J_{Pt-P}$ = 357 Hz, $^{2}J_{P-P}$ = 19.1 Hz, *P*(TMS)), 37.1 (d with satellite, $^{1}J_{Pt-P}$ = 2453 Hz, $^{2}J_{P-P}$ = 19.0 Hz, *P*Ph$_3$) ppm. $^{195}Pt\{^{1}H\}$ NMR (86.02 MHz, C_6D_6, 298 K): δ = 4653.5 (ddd, $^{1}J_{Pt-P}$ = 2466 Hz, 359.0 Hz). ^{195}Pt NMR (86.02 MHz, C_6D_6, 298 K): δ = 4653.4 (ddm, $^{1}J_{Pt-P}$ = 2459 Hz, 358.2 Hz, $^{3}J_{Pt-H}$ = 32.5 Hz). HRMS (APCI, toluene, *m*/*z*): calcd for $C_{39}H_{57}N_2P_2PtSi_3$, 894.2947; found, 894.2947.

Preparation of [LSi{Pt(PPh$_3$)}$_2$P(TMS)$_2$], 3. A solution of (η^2-C_2H_4)Pt(PPh_3)$_2$ (342 mg, 0.458 mmol) in toluene (5 mL) was added to a solution of **1** (100 mg, 0.229 mmol) in toluene (10 mL) at −30 °C. The solution turned to a brown color and was slowly warmed to room temperature for 3 h. After stirring at room temperature for 16 h, the filtrate was concentrated to approximately 1 mL. Upon the addition of hexane (9 mL) to the resulting red oil, **3** was obtained as a red-brown solid (190 mg, 0.141 mmol, 52%). Crystals suitable for single crystal X-ray analysis were grown from C_6D_6 at 4 °C. Mp 234−235 °C. ^{1}H NMR (400.13 MHz, C_6D_6, 298 K): δ = 0.46 (d, 18 H, $^{3}J_{P-H}$ = 5.2 Hz, P(*TMS*)$_2$), 0.92 (s, 18 H, C*Me*$_3$), 6.98−7.02 (m, 5 H, C*Ph*), 7.07−7.11 (m, 6 H, *p*-P*Ph*$_3$), 7.21−7.25 (m, 12 H, *m*-P*Ph*$_3$), 8.13−8.08 (m, 12 H, *o*-P*Ph*$_3$) ppm. $^{13}C\{^{1}H\}$ NMR (100.61 MHz, C_6D_6, 298 K): δ = 5.0 (d, $^{2}J_{C-P}$ = 11.1 Hz, *TMS*), 31.4 (C*Me*$_3$), 53.6 (C*Me*$_3$), 129.1, 129.3, 134.9, 141.4 (d of virtual triplets, P*Ph*$_3$), 128.6, 129.3, 130.0, 131.8 (C*Ph*), 164.1 (d, $^{4}J_{C-P}$ = 2.95 Hz, NCN) ppm. $^{29}Si\{^{1}H\}$ NMR (79.49 MHz, C_6D_6, 298 K): δ = 8.3 (d, $^{1}J_{P-Si}$ = 7.4 Hz, *TMS*), 234.5 (dt, $^{2}J_{P-Si}$ = 219.4 Hz, 48.5 Hz, *Si*Pt$_2$) ppm. $^{31}P\{^{1}H\}$ NMR (81.012 MHz, C_6D_6, 298 K): δ = 56.0 (d with two satellites, $^{2}J_{P-P}$ = 33.3 Hz, *P*Ph$_3$; first satellite $^{1}J_{Pt-P}$ = 5137 Hz, $^{2}J_{P-P}$ = 33.3 Hz, $^{3}J_{P-P}$ = 86.4 Hz; second satellite $^{2}J_{Pt-P}$ = 60.5 Hz, $^{2}J_{P-P}$ = 33.3 Hz, $^{3}J_{P-P}$ = 86.4 Hz), −94.6 (t with three satellites, $^{2}J_{P-P}$ = 33.3 Hz, *P*(TMS)$_2$; first satellite $^{1}J_{Pt-P}$ = 1633.0 Hz; second satellite $^{1}J_{Si-P}$ = 219.2 Hz; third satellite $^{1}J_{Pt-P}$ = 1633.0 Hz) ppm. $^{195}Pt\{^{1}H\}$ NMR (86.02 MHz, C_6D_6, 298 K): δ = −5171.5 (ddd with satellites, $^{1}J_{Pt-P}$ = 5136, 1633.0 Hz, $^{2}J_{Pt-P}$ = 60.0 Hz; $^{1}J_{Pt-Si}$ = 1117 Hz) ppm. Elemental Analysis: calcd for $C_{57}H_{71}N_2P_3Pt_2Si_3$: C, 50.65; H, 5.30; N, 2.07; found: C, 51.06; H, 5.30; N, 1.86. HRMS (APCI, toluene, *m*/*z*): calcd for $C_{57}H_{71}N_2P_3Pt_2Si_3$, 1350.3433; found, 1350.3462.

Preparation of [LSi{Pd(PPh$_3$)}$_2$P(TMS)$_2$], 4. A solution of phosphasilene **1** (65.5 mg, 0.15 mmol) in toluene (5 mL) was added to a suspension of Pd(PPh_3)$_4$ (347 mg, 0.30 mmol) in toluene (15 mL) at 0 °C. The reaction mixture was stirred at low temperatures for 1 h and was subsequently heated to 40 °C for 4 h. NMR spectroscopy and MS spectrometry showed the complete formation of **4**.

To phosphasilene **1** (45 mg, 0.10 mmol) and Pd(PPh_3)$_4$ (170 mg, 0.15 mmol) in a Young-NMR tube, THF-d_8 (0.6 mL) was added. This mixture was heated to 50 °C for 3 days to give a nearly complete conversion of **1** to **4**.

^{1}H NMR (400.13 MHz, C_6D_6, 298 K): δ = 0.54 (d, $^{3}J_{H-P}$ = 5.2 Hz, 18 H, *TMS*), 0.86 (s, 18 H, C*Me*$_3$), 8.10 (m, 12 H, *o*-P*Ph*$_3$) ppm. ^{31}P NMR (81.012 MHz, C_6D_6, 298 K): δ = 41.2 (d, $^{2}J_{P-P}$ = 11.2 Hz, *P*Ph$_3$), −163.4 (t, $^{2}J_{P-P}$ = 11.2 Hz, *P*(TMS)$_2$) ppm.

^{1}H NMR (400.13 MHz, THF-d_8, 298 K): δ = 0.13 (d, 18 H, $^{3}J_{P-H}$ = 4.9 Hz, *TMS*), 0.81 (s, 18 H, C*Me*$_3$) ppm. $^{13}C\{^{1}H\}$ NMR (100.61 MHz, THF-d_8, 298 K): δ = 6.2 (d, $^{2}J_{P-C}$ = 22.2 Hz, *TMS*), 31.9 (C*Me*$_3$), 54.1 (*C*Me$_3$), 128.7, 135.6, 138.6, 138.9 (PdP*Ph*$_3$) ppm. $^{29}Si\{^{1}H\}$ NMR (79.49 MHz, THF-d_8, 298 K): δ = 0.01 (d, $^{1}J_{P-Si}$ = 6.0 Hz, *TMS*), 187.8 (dt, $^{2}J_{Si\text{-}PPh_3}$ = 43.4 Hz, $^{2}J_{Si\text{-}PTMS_2}$ = 184.3 Hz, *Si*Pd$_2$) ppm. $^{31}P\{^{1}H\}$ NMR (81.012 MHz, THF-d_8, 298 K): δ = 38.0 (d, $^{2}J_{P-P}$ = 5.2 Hz, *P*Ph$_3$), −173.0 (t, $^{2}J_{P-P}$ = 5.2 Hz, *P*(TMS)$_2$) ppm. The proton and carbon NMR signals of the phenyl group in the ligand attached to silicon could not be assigned since they overlapped with the respective, more intense triphenyl phosphine NMR signals. HRMS (APCI, toluene, *m*/*z*): calcd for $C_{57}H_{72}N_2P_3Pd_2Si_3$, 1173.2222; found, 1173.2241.

Preparation of [{(LSi)$_2$P(TMS)}Ni(COD)], 5. A toluene solution (3 mL) of Ni(COD)$_2$ (55.0 mg, 0.20 mmol) was added to a solution of **1** (131 mg, 0.30 mmol) in toluene (6 mL) at ambient temperature. The solution turned to a brown color and was stirred for 14 h at 50 °C. The solution was filtered. The filtrate was concentrated and stored at −30 °C to yield **5** as red crystals (87 mg, 0.73 mmol, 73%). Mp 195−197 °C. ^{1}H NMR (200.13 MHz, C_6D_6, 298 K): δ = 0.57 (d, $^{3}J_{P-H}$ = 4.4 Hz, 9 H, *TMS*), 1.41 (s, 36 H, C*Me*$_3$), 2.73 (m, 4 H, C*H*$_2$ of COD), 2.89 (br, 4 H, C*H*$_2$ of COD), 4.79 (br, 4 H, C*H* of COD), 6.92−7.02, 7.22, 7.32 (m, 10 H, *Ph*) ppm. $^{13}C\{^{1}H\}$ NMR (100.61 MHz, C_6D_6, 298 K): δ = 4.3 (d, $^{2}J_{C-P}$ = 7.9 Hz, *TMS*), 31.5 (C*Me*$_3$), 33.5 (*C*H$_2$ of COD), 54.0 (*C*Me$_3$), 77.8 (*C*H of COD), 129.4, 129.5, 129.9, 134.0 (*Ph*), 165.2 (NCN) ppm. $^{29}Si\{^{1}H\}$ NMR (79.49 MHz, C_6D_6, 298 K): δ = 51.5 (d, $^{1}J_{P-Si}$ = 73.2 Hz, L*Si*) ppm. ^{29}Si-Inept (79.49 MHz, J_{Si-H} = 5 Hz, C_6D_6, 298 K): −9.2 (d, $^{1}J_{P-Si}$ = 75.8 Hz, *TMS*) ppm. $^{31}P\{^{1}H\}$ NMR (81.012 MHz, C_6D_6, 298 K): δ = −125.4 (satellite, $^{1}J_{Si-P}$ = 73.7 Hz) ppm. HRMS (APCI, toluene, *m*/*z*) calcd for $C_{41}H_{67}N_4NiPSi_3$, 788.3759; found, 788.3734.

Theoretical Calculations. Mechanistic investigation were carried out at the B97-D/cc-pVTZ/(SMD = toluene)//B97-D/6-31G* level of

dx.doi.org/10.1021/ja409720c | J. Am. Chem. Soc. 2013, 135, 17958−17968

theory (cc-pVTZ-PP on Pt and Pd atoms and cc-pVTZ on Ni atoms).[30] Stationary points on the potential energy surface (PES) were characterized by harmonic vibrational frequency calculations. Transition states, with one imaginary frequency, were confirmed by intrinsic reaction coordinate (IRC) calculations. Analyses of molecular orbitals were carried out at the B3PW91/6-31G(d)/LANL2DZ [Pt] level of theory. The NBO approach was used to calculate the orbital populations, Wiberg bond indices (WBI), and natural population analysis (NPA). Calculations were carried out using the GAUSSIAN 09 program.[31]

■ ASSOCIATED CONTENT

Supporting Information

Details on X-ray crystal structure analyses, selected NMR and mass spectra of **2**−**5**, as well as additional data on the DFT calculations, NBO analyses, optimized structures, and more elaborate mechanistic schemes. This material is available free of charge via the Internet at http://pubs.acs.org.

■ AUTHOR INFORMATION

Corresponding Author

shigeyoshi.inoue@tu-berlin.de

Notes

The authors declare no competing financial interest.

■ ACKNOWLEDGMENTS

This work was supported by the Sofja Kovalevskaja Program (Alexander von Humboldt foundation). T.S. thanks the support of The New Széchenyi Plan TAMOP-4.2.2/B-10/1-2010-0009. We thank Carsten Eisenhut for his assistance with experimental work.

■ REFERENCES

(1) (a) Lee, V. Ya.; Sekiguchi, A.; Escudié, J.; Ranaivonjatovo, H. *Chem. Lett.* **2010**, *39*, 312−318. (b) Driess, M. *Coord. Chem. Rev.* **1995**, *145*, 1−25.

(2) Smit, C. N.; Lock, F. M.; Bickelhaupt, F. *Tetrahedron Lett.* **1984**, *25*, 3011−3014.

(3) (a) Smit, C. N.; Bickelhaupt, F. *Organometallics* **1987**, *6*, 1156−1163. (b) Niecke, E.; Klein, E.; Nieger, M. *Angew. Chem., Int. Ed. Engl.* **1989**, *28*, 751−752. (c) Driess, M. *Angew. Chem., Int. Ed. Engl.* **1991**, *30*, 1022−1024. (d) Corriu, R.; Lanneau, G.; Priou, C. *Angew. Chem., Int. Ed. Engl.* **1991**, *30*, 1130−1132. (e) Bender, H. R. G.; Niecke, E.; Nieger, M. *J. Am. Chem. Soc.* **1993**, *115*, 3314−3315. (f) Driess, M.; Rell, S.; Pritzkow, H. *J. Chem. Soc., Chem. Commun.* **1995**, 253−254. (g) Driess, M.; Pritzkow, H.; Rell, S.; Winkler, U. *Organometallics* **1996**, *15*, 1845−1855. (h) Yao, S.; Block, S.; Brym, M.; Driess, M. *Chem. Commun.* **2007**, 3844−3866. (i) Lee, V. Ya.; Kawai, M.; Sekiguchi, A.; Ranaivonjatovo, H.; Escudié, J. *Organometallics* **2009**, *28*, 4262−4265. (j) Cui, H.; Zhang, J.; Cui, C. *Organometallics* **2012**, *32*, 1−4. (k) Li, B.; Matsuo, T.; Hashizume, D.; Fueno, H.; Tanaka, K.; Tamao, K. *J. Am. Chem. Soc.* **2009**, *131*, 13222−13223.

(4) Driess, M.; Block, S.; Brym, M.; Gamer, M. T. *Angew. Chem., Int. Ed.* **2006**, *45*, 2293−2296.

(5) Li, B.; Matsuo, T.; Fukunaga, T.; Hashizume, D.; Fueno, H.; Tanaka, K.; Tamao, K. *Organometallics* **2011**, *30*, 3453−3456.

(6) Hansen, K.; Szilvási, T.; Blom, B.; Inoue, S.; Epping, J. D.; Driess, M. *J. Am. Chem. Soc.* **2013**, *135*, 11795−11798.

(7) Inoue, S.; Wang, W.; Präsang, C.; Asay, M.; Irran, E.; Driess, M. *J. Am. Chem. Soc.* **2011**, *133*, 2868−2871.

(8) A cationic silyliumylidene diiron complex: Kawano, Y.; Tobita, H.; Shimoi, M.; Ogino, H. *J. Am. Chem. Soc.* **1994**, *116*, 8575−8581.

(9) (a) Roscher, A.; Bockholt, A.; Braun, T. *Dalton Trans.* **2009**, 1378−1382. (b) Yamashita, H.; Kobayashi, T.-a.; Hayashi, T.; Tanaka, M. *Chem. Lett.* **1990**, 1447−1450. (c) Arii, H.; Takahashi, M.; Nanjo, M.; Mochida, K. *Dalton Trans.* **2010**, *39*, 6434−6440.

(10) Braddock-Wilking, J.; Corey, J. Y.; Trankler, K. A.; Xu, H.; French, L. M.; Praingam, N.; White, C.; Rath, N. P. *Organometallics* **2006**, *25*, 2859−2871.

(11) Sen, A.; Halpern, J. *Inorg. Chem.* **1980**, *19*, 1073−1075.

(12) (a) Weber, L.; Schumann, I.; Stammler, H.-G.; Neumann, B. *J. Organomet. Chem.* **1993**, *443*, 175−183. (b) Domńaska-Babul, W.; Chojnacki, J.; Matern, E.; Pikies, J. *Dalton Trans.* **2009**, 146−151.

(13) Moor, A.; Pregosin, P. S.; Venanzi, L. M. *Inorg. Chim. Acta* **1981**, *48*, 153−157.

(14) (a) Braddock-Wilking, J.; Corey, J. Y.; French, L. M.; Choi, E.; Speedie, V. J.; Rutherford, M. F.; Yao, S.; Xu, H.; Rath, N. P. *Organometallics* **2006**, *25*, 3974−3988. (b) Tanabe, M.; Ito, D.; Osakada, K. *Organometallics* **2008**, *27*, 2258−2267. (c) Tanabe, M.; Ito, D.; Osakada, K. *Organometallics* **2007**, *26*, 459−462. (d) Gallo, V.; Latronico, M.; Mastrorilli, P.; Nobile, C. F.; Suranna, G. P.; Ciccarella, G.; Englert, U. *Eur. J. Inorg. Chem.* **2005**, 4607−4616.

(15) (a) Tanabe, M.; Jiang, J.; Yamazawa, H.; Osakada, K.; Ohmura, T.; Suginome, M. *Organometallics* **2011**, *30*, 3981−3991. (b) Arii, H.; Takahashi, M.; Nanjo, M.; Mochida, K. *Dalton Trans.* **2010**, *39*, 6434−6440. (c) Alonso, E.; Forniés, J.; Fortuño, C.; Martín, A.; Orpen, A. G. *Organometallics* **2001**, *20*, 850−859.

(16) For a recent review, see: Blom, B.; Stoelzel, M.; Driess, M. *Chem.—Eur. J.* **2013**, *19*, 40−62.

(17) Zarate, E. A.; Tessier-Youngs, C. A.; Youngs, W. J. *J. Chem. Soc., Chem. Commun.* **1989**, 577−578.

(18) (a) Mitchell, G. P.; Tilley, T. D. *Angew. Chem., Int. Ed.* **1998**, *37*, 2524−2526. (b) Grumbine, S. D.; Tilley, T. D.; Arnold, F. P.; Rheingold, A. L. *J. Am. Chem. Soc.* **1993**, *115*, 7884−7885.

(19) (a) Feldmann, J. D.; Mitchell, G. P.; Nolte, J.-O.; Tilley, T. D. *J. Am. Chem. Soc.* **1998**, *120*, 11184−11185. (b) Gehrhus, B.; Hitchcock, P. B.; Lappert, M. F.; Maciejewski, H. *Organometallics* **1998**, *17*, 5599−5601. (c) Agou, T.; Sasamori, T.; Tokitoh, N. *Organometallics* **2012**, *31*, 1150−1154.

(20) (a) Jutzi, P.; Mix, A.; Rummel, B.; Schoeller, W. W.; Neumann, B.; Stammler, H.-G. *Science* **2004**, *305*, 849−851. (b) Driess, M.; Yao, S.; Brym, M.; van Wüllen, C. *Angew. Chem., Int. Ed.* **2006**, *45*, 6730−6733. (c) Xiong, Y.; Yao, S.; Inoue, S.; Irran, E.; Driess, M. *Angew. Chem., Int. Ed.* **2012**, *51*, 10074−10077. (d) Xiong, Y.; Yao, S.; Inoue, S.; Epping, J. D.; Driess, M. *Angew. Chem., Int. Ed.* **2013**, *52*, 7147−7150. (e) Filippou, A. C.; Lebedev, Y. N.; Chernov, O.; Straßmann, M.; Schnakenburg, G. *Angew. Chem., Int. Ed.* **2013**, *52*, 6974−6978.

(21) (a) Inoue, S.; Epping, J. D.; Irran, E.; Driess, M. *J. Am. Chem. Soc.* **2011**, *133*, 8514−8517. (b) Blom, B.; Enthaler, S.; Inoue, S.; Irran, E.; Driess, M. *J. Am. Chem. Soc.* **2013**, *135*, 6703−6713.

(22) Yeong, H.-X.; Xi, H.-W.; Li, Y.; Lim, K. H.; So, C.-W. *Chem.—Eur. J.* **2013**, *19*, 11786−11790.

(23) (a) Fürstner, A.; Krause, H.; Lehmann, C. W. *Chem. Commun.* **2001**, 2372−2373. (b) Tanabe, M.; Takahashi, A.; Yamada, T.; Osakada, K. *Organometallics* **2013**, *32*, 1815−1820.

(24) Compare ^{1}H NMR (C_6D_6): δ = 0.06 ppm and ^{31}P NMR (C_6D_6): δ = −251.6 ppm in Holz, J.; Zayas, O.; Jiao, H.; Baumann, W.; Spannenberg, A.; Monsees, A.; Riermeier, T. H.; Almena, J.; Kadyrov, R.; Börner, A. *Chem.—Eur. J.* **2006**, *12*, 5001−5013.

(25) Wang, W.; Inoue, S.; Yao, S.; Driess, M. *J. Am. Chem. Soc.* **2010**, *132*, 15890−15892.

(26) As recent examples of bis(silylene) transition metal complexes with chelate ligand: (a) Wang, W.; Inoue, S.; Enthaler, S.; Driess, M. *Angew. Chem., Int. Ed.* **2012**, *51*, 6167−6171. (b) Brück, A.; Gallego, D.; Wang, W.; Irran, E.; Driess, M.; Hartwig, J. F. *Angew. Chem., Int. Ed.* **2012**, *51*, 11478−11482. (c) Wang, W.; Inoue, S.; Irran, E.; Driess, M. *Angew. Chem., Int. Ed.* **2012**, *51*, 3691−3694.

(27) Denk, M.; Hayashi, R. K.; West, R. *J. Chem. Soc., Chem. Commun.* **1994**, 33−34.

(28) (a) Meltzer, A.; Präsang, C.; Milsmann, C.; Driess, M. *Angew. Chem., Int. Ed.* **2009**, *48*, 3170−3173. (b) Meltzer, A.; Inoue, S.; Präsang, C.; Driess, M. *J. Am. Chem. Soc.* **2010**, *132*, 3038−3046.

(29) Sheldrick, G. M. *SHELX-97 Program for Crystal Structure Determination*; Universität Göttingen: Göttingen, Germany, 1997.

(30) (a) Frisch, M. J.; Pople, J. A.; Binkley, J. S. *J. Chem. Phys.* **1984**, *80*, 3265−3269. (b) Dunning, T. H. *J. Chem. Phys.* **1989**, *90*, 1007−1023. (c) Vahtras, O.; Almlöf, J.; Feyereisen, M. W. *Chem. Phys. Lett.* **1993**, *213*, 514−518. (d) Becke, A. D. *J. Chem. Phys.* **1997**, *107*, 8554−8560. (e) Grimme, S. *J. Comput. Chem.* **2006**, *27*, 1787−1799.

(31) Frisch, M. J.; Trucks, G. W.; Schlegel, H. B.; Scuseria, G. E.; Robb, M. A.; Cheeseman, J. R.; Scalmani, G.; Barone, V.; Mennucci, B.; Petersson, G. A.; Nakatsuji, H.; Caricato, M.; Li, X.; Hratchian, H. P.; Izmaylov, A. F.; Bloino, J.; Zheng, G.; Sonnenberg, J. L.; Hada, M.; Ehara, M.; Toyota, K.; Fukuda, R.; Hasegawa, J.; Ishida, M.; Nakajima, T.; Honda, Y.; Kitao, O.; Nakai, H.; Vreven, T.; Montgomery, J. A., Jr.; Peralta, J. E.; Ogliaro, F.; Bearpark, M.; Heyd, J. J.; Brothers, E.; Kudin, K. N.; Staroverov, V. N.; Kobayashi, R.; Normand, J.; Raghavachari, K.; Rendell, A.; Burant, J. C.; Iyengar, S. S.; Tomasi, J.; Cossi, M.; Rega, N.; Millam, J. M.; Klene, M.; Knox, J. E.; Cross, J. B.; Bakken, V.; Adamo, C.; Jaramillo, J.; Gomperts, R.; Stratmann, R. E.; Yazyev, O.; Austin, A. J.; Cammi, R.; Pomelli, C.; Ochterski, J. W.; Martin, R. L.; Morokuma, K.; Zakrzewski, V. G.; Voth, G. A.; Salvador, P.; Dannenberg, J. J.; Dapprich, S.; Daniels, A. D.; Farkas, Ö.; Foresman, J. B.; Ortiz, J. V.; Cioslowski, J.; Fox, D. J. *Gaussian 09*, Revision A.1; Gaussian, Inc.: Wallingford, CT, 2009.